Chemistry in light-induced 3D printing

(Article begins on next page)

17 October 2023

LECTURE TEXT

Chemistry in light-induced 3D printing

Alejandra Salas[1] · Marcileia Zanatta[2] · Victor Sans[2] · Ignazio Roppolo[1]

Abstract

In the last few years, 3D printing has evolved from its original niche applications, such as rapid prototyping and hobbyists, towards many applications in industry, research and everyday life. This involved an evolution in terms of equipment, software and, most of all, in materials. Among the different available 3D printing technologies, the light activated ones need particular attention from a chemical point of view, since those are based on photocurable formulations and in situ rapid solidification via photopolymerization. In this article, the chemical aspects beyond the preparation of a formulation for light-induced 3D printing are analyzed and explained, aiming at giving more tools for the development of new photocurable materials that can be used for the fabrication of innovative 3D printable devices.

Graphical abstract
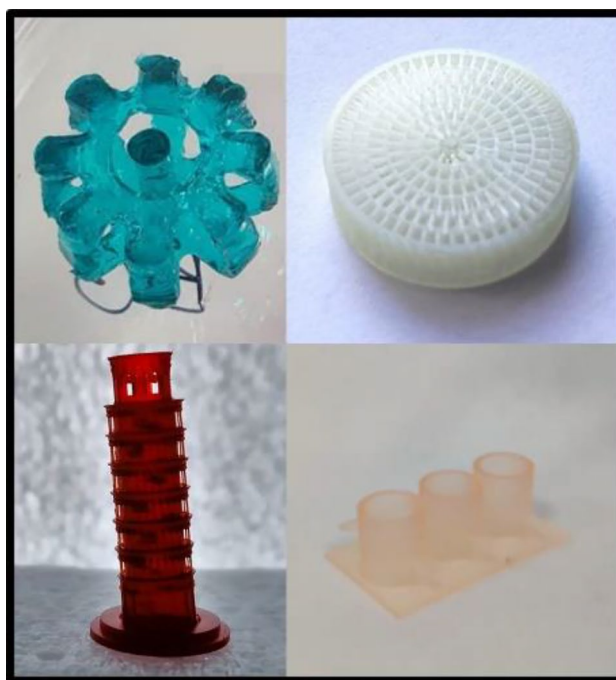
✉ Ignazio Roppolo
   ignazio.roppolo@polito.it

1 Department of Applied Science and Technology, Politecnico Di Torino, Corso Duca Degli Abruzzi 24, 10129 Turin, Italy

2 Institute of Advanced Materials (INAM), Univesitat Jaume I, Avda Sos Baynat S/N, 12071 Castellón, Spain

Introduction

Three-dimensional printing (3DP), the common name employed for polymeric additive manufacturing (AM), has emerged in the last decade as an advanced and versatile

technology that enables a rapid, personalized and on-demand fabrication of parts and objects. Currently, 3DP is one of the most promising manufacturing technologies, gaining more importance both in research and in industry [1]. Unlike in traditional manufacturing processes, using 3DP it is possible to fabricate almost any arbitrarily complex shapes, with very few limitations. The general concept is a build-up process which starts from a digital model (computer-aided design files or CAD) of the geometry to be fabricated. This file is then divided in slices by a dedicated software and sent to the 3D printer, which reproduces the object typically in a layer-by-layer fashion. This computer-aided manufacturing (CAM) has a high degree of automation and reproducibility, allowing precise control over the production [2].

Nowadays, there are several 3D printing technologies available. They are usually classified according to the raw material employed and/or by the operating principles through which the layers are created. According to the American Society for Testing and Materials (ASTM), there are more than 50 different AM technologies that can be classified into seven different categories: material extrusion, material jetting, binder jetting, sheet lamination, vat photopolymerization, powder bed fusion and direct energy deposition [3]. These techniques rely on different characteristics of the printer and fabrication parameters, which influence the model design and topological optimization, and determine the object resolution and production times, with a different characteristic in terms of the size of the features at various scales [4].

Being related to virtual models, 3DP enables the on-demand fabrication of customized products in a cost-effective manner, especially for limited productions, due to the ease modification of digital files. The modifications can be then spread virtually, enabling distributed fabrication, saving on time and transportation costs [5]. In addition to these advantages, there are environmental benefits such as lower energy consumption for small-batch productions and more efficient material use, since waste is extremely limited by the possibility of reusing almost all the feeding material. However, drawbacks related to the suitability, toxicity and sustainability of materials still need to be fully addressed [6].

On the other hand, 3DP still did not reach its premises. To do so, it is necessary to re-think the way products are designed and manufactured, gathering a controlled spatial arrangement to achieve hierarchical and intricate architectures, with graded or multi-material structures [7]. Thus, more efforts should be devoted to equipment improvement: 3DP can be slower compared with conventional processing, but it is more versatile and agile since it relies on single-step fabrication of a near-net shape object. This reduces the number of processing and post-processing steps required to achieve the final component, leading to a significant reduction in the overall operational time [8].

The major challenge nowadays is the limited availability of materials specifically designed for 3DP, since their development did not keep pace with the evolution of the techniques [9]. In the last decade, novel materials have been developed for processing via 3D printing and provide advanced properties to the final object. The combination of additive manufacturing and functional properties, such as stimuli responsiveness, is called 4D printing and is aimed at integrating specific structures and smart functionalities to enable applications in advanced fields such as medicine and aerospace [10]. In this context, chemistry is fundamental for the evolution of novel materials. Among the different 3DP techniques, light-induced 3DP (alternatively called vat polymerization 3D printing, VP 3DP) better matches chemical background with technological development.

For these reasons, this article is focused on showing the chemistry beyond light-induced 3DP, highlighting different aspects that are focus of current research, thus giving the tools for further advancements. First, the 3D printing techniques will be briefly described, focusing on the basis of photopolymerization. Afterwards, the single materials elements will be discussed, with particular focus on the chemical aspects.

VAT polymerization

Vat polymerization (VP) is an AM technology, in which a photopolymerization occurs in a tank of resin, commonly known as a vat, containing a formulation of monomers, additives, photoinitiators and fillers, detailed in the following sections [11]. The set-up includes a light source that photopolymerizes layer by layer a digital 3D design. Compared with other commonly employed AM techniques such as Fused Filament Fabrication (FFF), VP can achieve high printing resolution and accuracy, faster printing times and has the ability to tailor the formulations and consequently the properties of the materials fabricated.

VP techniques based on stereolithography (SL) processes were first developed in the early 1980s by Hideo Kodama and Charles Hull [12, 13]. SL is based on the focused polymerization of a thin layer of ink inside the vat by means of a laser beam. Afterwards, different related methodologies were developed, including digital light processing (DLP) [14, 15], micro-stereolithography (μSL) [16], continuous liquid interface production (CLIP) [17, 18], two-photon polymerization (2PP) [19] and computed axial lithography (CAL) [20]. A scheme of these techniques is depicted in Fig. 1.

The spatiotemporal-controlled photoactivated polymerization process enables precise over control the localized solidification of resin materials, which results in high shape fidelity of the final object compared with the digital model. The printing resolution on the *XY* plane, perpendicular to
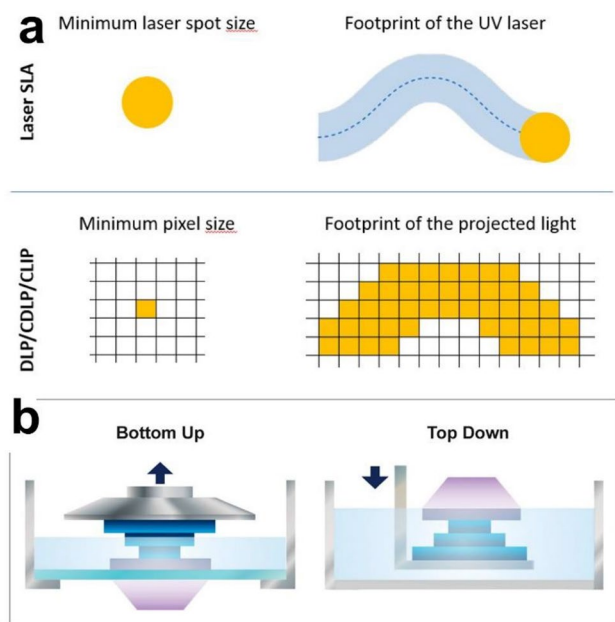
Fig. 1 SL-based technologies. **a** Methodologies to solidify the photopolymer resins in laser-based SL and in digital light projection technologies. Reprinted from [11]. **b** Bottom-up versus top–down vat technologies. Adapted with permission from [52]

the light irradiation, and in the vertical direction parallel to the irradiation path outlines the minimum volume unit, or voxel, that can be resolved. In SL machines, the solidified polymer is typically formed by focusing the laser using a galvanometric head on a building platform to create the first layer [21]. This polymerized layer remains attached to the building platform. After one layer has been cured, the platform is raised or lowered depending on the printing configuration. The resin optical transparency and therefore the light penetration is an important factor to determine the step size, which should be sufficient for the entire layer to be cured but not too small to avoid a curing depth beyond the desired layer height, which would lead to over-curing and ultimately lower the resolution of the printed parts. Layer thickness and irradiation times are key parameters that need to be carefully selected and optimized. The Z-axis steps should be selected to reach a compromise between high resolution and short build times. The vertical resolution depends mainly on the precision of the stepper motor screw of the printer and the mechanical accuracy of its rotation screw that controls the motion of the building platform [22]. However, other printing parameters affect the resolution on the Z axis, including the power and wavelength of the incident light. The subsequent layers are polymerized following the same procedure until the complete fabrication of the object. It is usual to have longer polymerizations times for the first layers, to ensure a robust binding to the platform. After the printing is complete, washing with alcohols (e.g. ethanol, isopropanol)

and post-curing processes are typically applied to remove non-polymerized resin and to improve the mechanical properties of the fabricated parts. The post-curing enhances the long-term structural stability of the printed structure because it increases the final cross-linking density, thus increasing the degree of polymerization, since the printing is performed to reach the gel point without inducing complete conversion of the resins [23]. SL machines that can be configured for the building platform to rise (bottom up) or lower (top down) (Fig. 1a). The light comes from the opposite direction to the movement of the platform. In the top-down configuration, the platform and printed part are submerged in the vat during the printing process. The light source is situated above the vat and the reaction occurs on the free surface [24]. For each cured layer, the object descends into the liquid precursor to coat another fresh uncured layer above it, and this requires deep tanks and large volumes of resin. In the bottom-up configuration, the laser beam hits the resin from the bottom of the vat through a transparent window, and the object remains attached to the platform that rises according to the formation of each layer. This is normally preferred, since it reduces the volume of resin required, especially to build large parts and it is not dependent on the vat depth, which limits the size of the printable geometries. In SL, the laser spot size determines the XY resolution achievable. Classic SL technology can achieve ca. 10 μm XY resolution [25].

In the early 1990s, micro-stereolithography AM (MSL or μSL) was developed, with the main difference compared with SL in the laser spot size of about 5 μm [16]. Recently, the use of more precise lasers has allowed the generation of structures with submicron features [26]. Digital light processing (DLP) 3D printers direct the light with deformable mirror device (DMD) chips [27, 28]. Here, each micro-mirror on the DMD represents one pixel from the digital image in the layer to be solidified. Under optimized conditions, printing resolutions of 3–5 μm in the XY plane can be achieved [29]. For each layer printed, the entire cross-section of the object is projected, which is significantly faster than the single-point laser SL technology. Indeed, the photopolymerization of the entire cross-section of the object significantly reduce printing times compared with SL techniques, and enables printing of larger areas. Currently, the best commercial DLP-based printers claim resolutions of about 20 μm [30]. Recently, another technology has gained enormous commercial interest due to its simplicity and low cost, while maintaining resolutions close to DLP. They use a light-emitting diode (LED) array, usually at 405 nm, as a light source and a liquid-crystal display (LCD) screen to act as a mask that directs the layer polymerization. These technologies are very affordable and can achieve high resolutions (28×28 μm) dictated by the LCD screen resolution, rapid printing times (1–3 s/layer) and high build volumes [31]. A breakthrough in the

field was reported in 2015, when the continuous liquid interface production (CLIP) was reported [32]. Here, a thin interfacial layer of oxygen is created at the bottom of the vat through an oxygen-permeable window. The oxygen acts as a polymerization inhibitor in the window surface, allowing a continuous interface for polymerization, very near the bottom window. This results in a 'layer-less' printing and therefore considerably increases the printing speed (500 mm/h). An added advantage of this technology is that the parts fabricated are considerably more isotropic than other SL techniques due to the layer-less nature. Recently, the group of Prof. Mirkin reported a breakthrough that permits the area of printing and the speed to be increased, branded high-area rapid printing (HARP) [32]. A flow of a thin layer of fluorinated oil employed in the base of the printing bed avoids the adhesion of the materials to the base and facilitates the continuous cooling in the printing front. This helps dissipate the heat generated during the polymerization. This technique allows to fabricate multiple materials beyond photopolymers, including elastomers, ceramics and thermoplastics.

Other niche applications have also been developed, namely two-photon polymerization (2PP) and computed axial lithography (CAL). The main feature of 2PP is that the process is activated by the simultaneous absorption of two photons generated by a pulse of a pico- or femtolaser pulse [33]. The absorption happens in the more energetic part of the laser spot, which starts the free-radical polymerization, resulting in structures in the range of 100 nm. [15, 33] Despite the impressive resolutions achievable, 2PP suffers from important drawbacks for industrial implementation including the high cost of the equipment, the limited building volume (< 1 mm in height) and the low printing velocity, typically in the range of 0.5–1 mm/s. Computed axial lithography (CAL) was developed at Lawrence Livermore National Laboratory and is a volumetric 3D printing technique, in contrast to traditional 'layer-by-layer' approach. CAL employs computed tomography (CT) images to generate a hologram within a controlled photopolymer volume. This hologram is generated by the simultaneous projection of several 2D images while the vat tank rotates continuously. The images combine through the liquid resin from different angles, resulting in a three-dimensional hologram with enough energy to photopolymerize a volume of resin. The key parameters of CAL techniques are the angular velocity and the resins' viscosity. The speed of rotation has an impact on the printed features, if it is too fast and viscosity must be enough to prevent a relative the relative shift of the 3D printed model and the rest of the liquid resin. CAL present some interesting features, including high production speed, since it works volumetrically and has high surface definition.

Principle of photopolymerization and influence of light absorbers

Photopolymerization is a polymerization method that basically employs the energy provided by photons (i.e. light) to initiate the reaction. Different from other polymerization methods, photopolymerization can occur only by polyaddition, with the continuous reaction of propagating species (radical of cation) with unreacted monomers. This reaction brings about the formation of polymer chains and, consequently, polymeric materials [34].

A photopolymerization reaction is typically divided into three steps:

- Initiation, i.e. the step in which light generates the active species;
- Propagation, i.e. the step in which photogenerated species react with monomers, leading to an increase in molecular weight and the formation of the polymeric chains or networks;
- Termination, i.e. the step in which the polymerization reaction ends, for multiple reasons [35].

Thus, the first necessary step to induce photopolymerization is the generation of reactive species, which is induced by the light. This can happen only employing chemical compounds, called photoinitiators, which are able to absorb the light radiation and consequently generate the initiating species. This can occur by direct generation of the reactive species (Norrish I photoinitiators) or aided by a co-initiator (Norrish II photoinitiators). The photochemical mechanisms beyond these two types of photoinitiators have already been explored[36, 37], but for the sake of clarity they are summarized here. In Norrish I photoinitiators, the absorbed light excites the molecule to a triplet state, which then decays to a singlet state, with consequent cleavage of a σ-bond and generation of two radicals, able to initiate the polymerization reaction. Differently, in Norrish II photoinititiators, the excited molecule abstracts an H atom from a donating co-initiator (usually amines), decaying to equilibrium state, whereas the co-initiator can now start the polymerization. In any case, independently from the path, the initiation mechanism can be shown as follows (Eq. 1):

$$PI \xrightarrow{h\nu} R \cdot R_i = \Phi_i I_z \varepsilon [PI] \tag{1}$$

where R_i is the initiation rate, Φ_i is the initiation quantum yield, ε is the molar extinction coefficient at a given wavelength, [PI] the molar concentration of the photoinitiator and I_z is the incident photonic flux. This coefficient is related to the incident radiation I_o (i.e. the radiation at the surface) through the equation (Eq. 2)

$$I_Z = I_o\left(10^{-A}\right) \tag{2}$$

where A (the absorbance) is defined by the Lambert Beer law (Eq. 3)

$$A = \varepsilon z c \tag{3}$$

where c is the concentration of the absorbing species, that in the present case is the concentration of the photoinitiator. Consequently, the initiation rate (i.e. the efficiency of polymerization starting) is related to both the chemical characteristics of the photoinitiator (via Φ_i) and the light intensity. On the other hand, it also emerges that given a certain light source (i.e. fixed I_o), increasing the photoinitiator concentration [PI], the penetration length of the light (z) decreases. In VP 3D printing, where Z steps are fixed by the operator (i.e. slicing), this is of particular importance, since the control of the penetration allows both an efficient adhesion of the different layers and a more precise printing, avoiding uncontrolled polymerization beyond the desired voxel.

The second step of photopolymerization, propagation, starts when an initiating species R· reacts with a monomer (M), thus generating a propagating reactive group which, interacting with other monomers, leads to the growing polymeric chain (P). This process is described by the following equation (Eq. 4) but

$$R^\cdot + M \rightarrow RM^\cdot \xrightarrow{M} P^\cdot \quad R_p = k_p[P^\cdot][M] \tag{4}$$
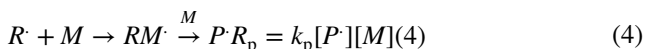
where R_p is the rate of polymerization and k_p is the constant of chain propagation.

In most cases, in photopolymerization this polyaddition propagating reaction is a chain-grow mechanism, typical of unsaturated bonds (vinyl, acrylate, methacrylate, etc.) or rings (epoxy, etc.). An alternative to this mechanism is step-growth polymerization, which is typical of thiol-ene/-yne photopolymerization reactions; the kinetics of this polymerization mechanism is out of the scope of this article, but it can be found described in detail in the literature [38]. The extent of the propagation step determines the molecular wight, which in turn determines many parameters such as the gel-point, and the mechanical and physiochemical properties of the polymer. The relationships between these properties have been reported in the literature [39, 40], but it is worthy to mention some aspects directly related to light-induced 3D printing. Fast kinetics and rapid gelling of the formulation imply a shorter irradiation time, which is preferred to decrease printing times and to increase precision, since after gelling, propagating species hardly proceed. For that reason, in light-induced 3D printing, multifunctional monomers are employed, which generates highly cross-linked polymers with rapid gelification and (theoretically) infinite molecular weight. Furthermore, mono-funtional monomers lead to linear

polymers, which are generally soluble in their monomers, disabling the possibility of obtaining solid objects. Most of the 'standard' commercial resins for VP 3D printing have these characteristics since the priorities were rapid printing and extreme precision. Nowadays, many resins with different characteristics are developed for light-induced 3D printing, with different mechanical and physico-chemical properties (discussed below).

Finally, termination of the polymerization occurs when two growing polymeric chains react, following this mechanism (Eq. 5)

$$P^\cdot + P^\cdot \rightarrow \text{Polymer} \quad R_t = k_t[P^\cdot]^2 \tag{5}$$
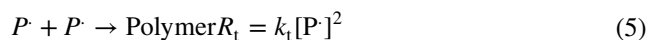
where R_t is the rate of termination and k_t is the kinetics constant of the reaction. By combining these relations, the rate of polymerization can be expressed as (Eq. 6)

$$R_p = \frac{k_p}{k_t^{0.5}}\left[R_i\right]^{0.5}[M] \tag{6}$$

This equation was demonstrated to be particularly valid for mono-functional monomers. When termination occurs mainly for kinetics effect, related to the decrease of the mobility of the species in the polymeric network, which is typical for 3D photopolymerization, a modification of this kinetics equation is necessary, as demonstrated in the literature [34]. Notably, the polymerization kinetics is proportional to the first power of the concentration of monomers and to the square root of light intensity. Thus, the quantum yield of the polymerization Φ_P results (Eq. 7)

$$\Phi_P = \frac{R_P}{I_z} \tag{7}$$

which clearly decreases increasing light intensity. In addition, Eq. 5 shows that the termination rate is proportional to the power of two to the concentration of the propagating macro-molecular species ($P^\cdot$), which depends on the concentration of the initiating species. Consequently, it is necessary to limit the photoinitiator concentration, since on one side it speeds up polymerization but on the other side, if in excess, leads to high termination [41].

While in many applications of photopolymerization it is 'simply' necessary to have a fast and effective polymerization, in 3D printing it is also necessary to have spatial control over the polymerization, to obtain precise structures [42, 43].

In most cases, the resolution is empirically obtained by adjusting the quantity and type of the photoinitiator and the printing parameters, such as layer exposure time and light intensity. In addition, other important parameters that affect the rate of polymerization are the monomer reactivity and the temperature.

Two strategies can be applied to increase precision in 3D printing. The first one involves the use of dyes and photoabsorbers, i.e. molecules able to absorb the light in the same spectral range of photoinitiators, but without generating reactive species. In this case, the absorbance of a formulation (A_f) can be described as (Eq. 8)

$$A_f = z \sum \varepsilon_i c_i \tag{8}$$

where A_f at a given wavelength with a given optical path length (z) is simply the sum of the contributions of the concentration (c_i) of every absorbing species i multiplied for the corresponding coefficient of its molar extinction (ε_i). Dyes, competing with the photoinitiator in photon absorption, increase the absorbance and, in turn, decrease the rate of initiation (Eq. 1) with obvious consequences on the photopolymerization mechanism. In this context, the dyes in VP 3D printing allow a finer control on the XY plane, decreasing propagation out of the pixel of irradiation [44].

Furthermore, the following equation must be taken into consideration (Eq. 9)

$$C_d = D_p \ln\left(\frac{E_{MAX}}{E_c}\right) \tag{9}$$

where the C_d is the curing depth, D_p the light penetration depth, E_{MAX} the energy dosage per units of area and E_c is the 'critical' energy to activate the reaction. D_p is empirically defined as (Eq. 10)

$$D_p = \frac{1}{2.3\varepsilon[PI]} \tag{10}$$

So, inversely proportional to ε and to the concentration of photoinitiator, it thus emerges that the presence of dyes increases the coefficient of molar extinction and decreases the curing depth. In this respect, dyes allow the precise control of C_d which, in principle, should be as close as possible to the Z step of the 3D printing process. [42, 45, 46]

The second approach involves the use of scavengers, in particular radical scavengers. These chemical compounds are able to trap radicals, thereby stabilizing them. It emerges that in a radical photoinduced process, radical scavengers may react both with initiating species (Eq. 1) and with propagating species (Eq. 4), inducing termination (Eq. 5). If on the one hand radical scavengers reduce the speed of the 3D printing process by decreasing the rate of the polymerization, which in turn implies longer irradiation times per layer, on the other hand they can interact with growing macro-molecules, that are generated in the irradiated voxels and then propagate out of those, stopping the polymerization [47, 48]. A balanced introduction of radical scavengers can thus slightly affect the

polymerization rate but efficiently end propagation, confining polymerization in the irradiated area and increasing resolution.

3D printable formulations

A common photocurable formulation, suitable for all the above-mentioned 3D printing technologies, is composed of at least two components: monomers/oligomers and photoinitiator(s) (PI) [49, 50]. Independently of the technology or polymerization mechanism, resins could also contain other ingredients that can enhance their printability or provide specific properties, such as radical scavengers, dyes and fillers or additives.

As mentioned in the previous sections, the VP process starts with a patterned exposure to light that activates the PI, which absorbs the incident radiation and generates reactive species, usually radicals, encouraging the conversion of the liquid monomers into a cured covalent network [51]. This PI must be compatible with the corresponding light source, commonly UV or visible light, the latter being much safer and compatible with cell-laden water-based inks [52, 53]. On the other hand, photocurable species, such as monomers or oligomers have single or multiple active groups, as side or chain-ends, that enable their association into a cross-linked network predominantly on the irradiated regions [54]. Therefore, for an accurate 3D printable formulation, there should be tuning between the composition and the properties, which in turn define the curing kinetics and penetration depth. These, combined with adequate printing parameters such as light intensity and time exposure, allows an optimized VP regarding the curing speed, precision and mechanical integrity.

In all these light-based technologies, the polymerized object has continuous contact with the liquid resin, therefore it must not be soluble in the ink during the printing. This condition is achieved by supplying enough energy to reach the material's gel point [55]. In the next sections, the chemistry of the main components of a 3D printable formulation will be introduced.

Monomers

Free-radical polymerizable resins are frequently based on the highly reactive (meth) acrylate functionalities [56]. These groups are employed as building blocks to develop bigger molecules due to their high reactivity upon light irradiation, well-established mechanisms and commercial availability [57]. A few examples of the most common monomers and oligomers according to their nature are shown in Fig. 2. Other functionalities can also be used, such as polyester, vinyl, vinyl ether, thio-ene/yne and even cationic-based
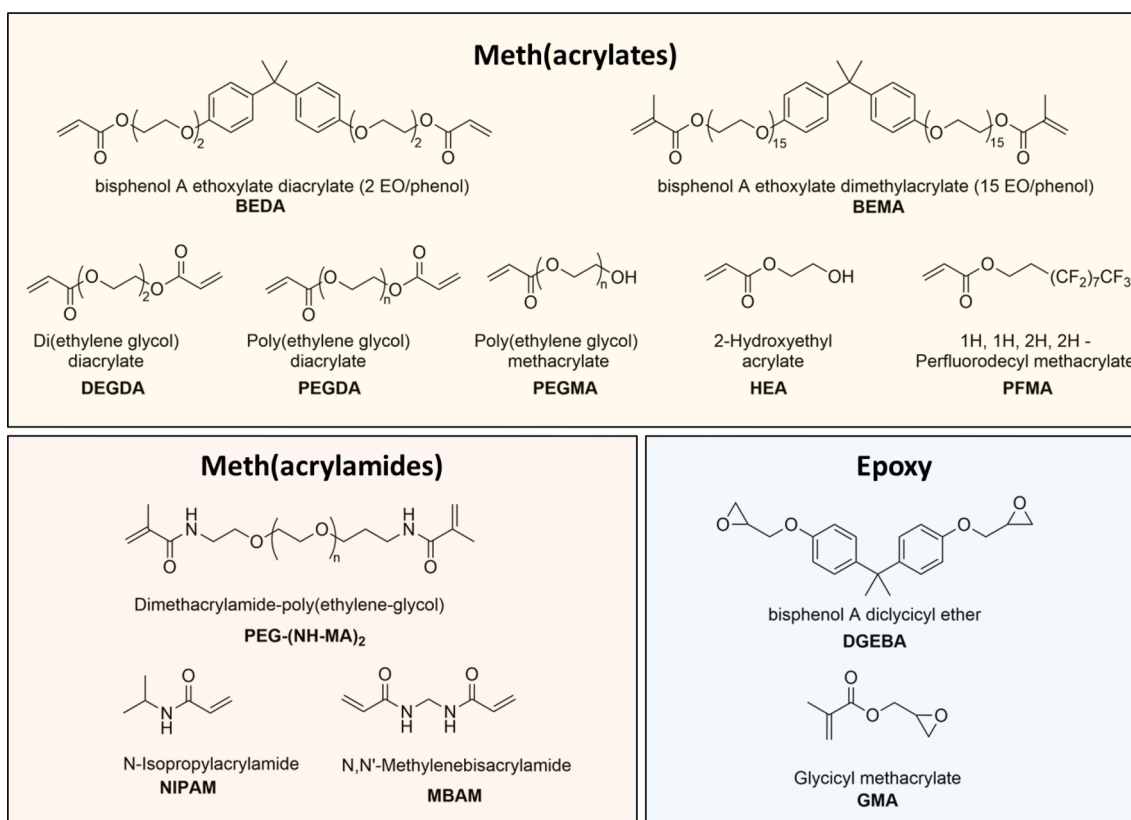
Fig. 2 Chemical structure of commercially available polymers and monomers for application in 3D printing

systems (combining free radical systems) [58–61]. The selection of suitable monomers or oligomers for VP is based on the application and processing technology to be used.

The main criteria for their selection are functionality (mono-, di- or poly-), viscosity, reaction kinetics, hydrophobicity/hydrophilicity, shrinkage, costs, shelf life, volatility, toxicity and the final mechanical and functional characteristics of the product [54]. However, commercially available resins are based on the optimum criteria for printing according to the chosen technology, but their formulation tends to be a selection of multifunctional monomers that are usually not explained in detail.

For the selection of monomers in a photocurable formulation, it is necessary to know that the reactive groups mainly control the kinetics, while the backbone mainly influences the physicochemical and mechanical properties (strength, brittleness and hydrophilicity) of the polymer [62].

The preference for acrylates is due to their fast reactivity related to their chain growth-polymerization mechanism (Fig. 3a) and oxygen inhibition, that allows good adhesion between printing layers[54]. However, they tend to shrink when cured, leading to poor resolution, internal stress or even damage to printed objects. Meanwhile, methacrylate monomers reduce the shrinkage problem but with a slower curing rate. Aromatic or high-molecular-weight (meth)

acrylates are characterized instead by lower shrinkage and adequate kinetics. [30, 63–66]

Other monomers with a wide range of functional groups have been reported, including (meth)acrylamides, which are compatible with different AM technologies (Fig. 3b). The reactivity of these moieties decreases together with the inductive effect, this way, the methyl-functionalized molecules also have a lower tendency to homopolymerization. Therefore, reactivity can be modulated by electron acceptor groups that impart stability to intermediate radical species [67]. Furthermore, molecules with a polymerizable double bond, such as methacryloyl groups can be used on the backbone of an unreactive species, by esterification of hydroxy or amino groups to provide photoreactivity [68]. This method enables the functionalization of natural (e.g. gelatin, chitosan or cellulose) and synthetic polymers [23].

On the other hand, reactivity also depends on the number of present functionalities in the reactive species. As multiple functionalities lead to an auto-acceleration in the early phases of the propagation, a higher viscosity and a denser and stiffer network, which would mean a considerable amount of unreacted double bonds [52]. Monomer molecular weight has a great impact on this phenomenon, as low-molecular-weight species have lower viscosities and increased mobility while higher-molecular-weight
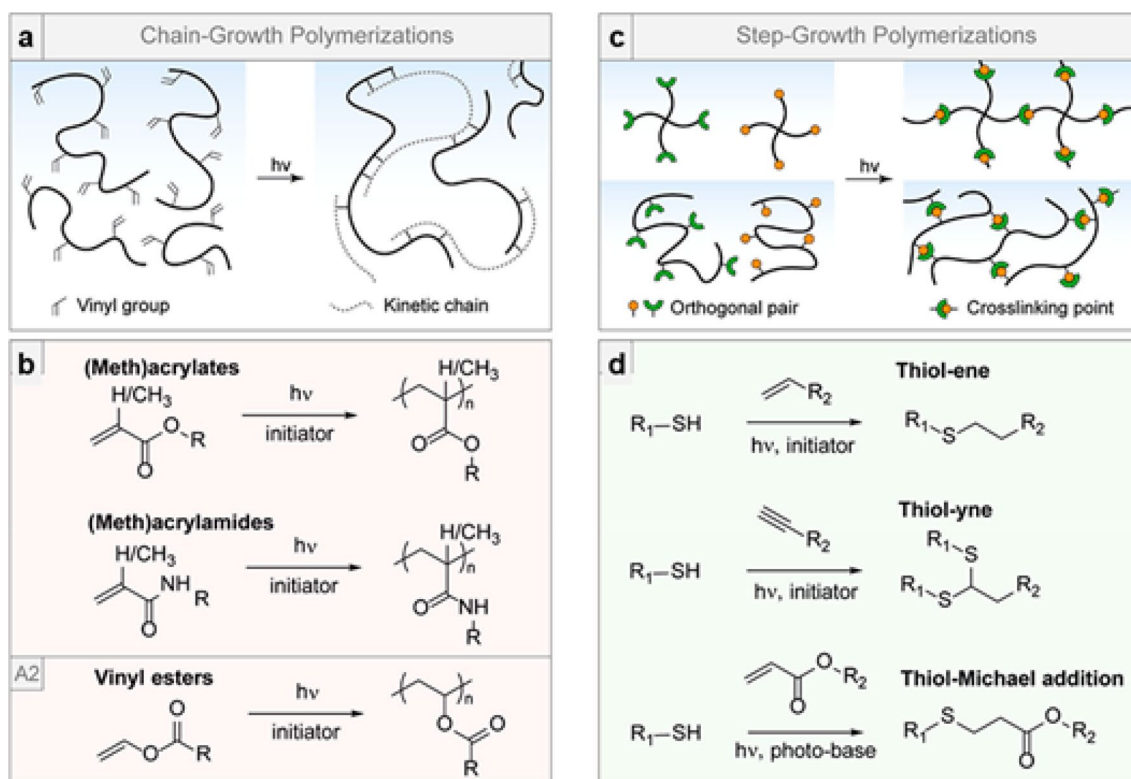
Fig. 3 Schematic representation of photopolymerization mechanisms. **a** Chain growth and **b** examples of reactions of various reactive species. **c** Step-growth polymerization mechanisms, **d** examples for various reactive species. Reprinted with permission from [52]

monomers can reduce shrinkage but restrict mobility and viscosity, requiring a diluent. Also, as mentioned, the backbone influences the mechanical stress and properties of the final polymer. The propagation has diffusion-controlled kinetics, where limited mobility of the macro-radical chain ends produces a heterogeneous network with highly and loosely cross-linked regions [69].

For more niche applications, thiol-ene/-yne systems and epoxy are also used in VP, known for their reduced shrinkage, lower stress and higher conversion compared with acrylate [60, 66, 70]. C–S–C bonds in thiol-enes implies low mechanical properties, but this can be overcome by adding allyl ethers to the mixtures. [66] Furthermore, an increase in the glass transition temperature of the polymers can be obtained by replacing alkene with an alkyne in the mixtures with thiols monomers, because of the increase of cross-linking density in the network [30]. Thiol-ene polymerization follows a step-growth pathway, as depicted in Fig. 3c, requiring a PI instead of a chemical catalyst [52, 71]. The advantages of thiol-ene networks include their high rate of reaction and conversion under ambient conditions, with reduced shrinkage due to the delay in the gel point and mechanical stress, as well as their lower susceptibility to oxygen inhibition compared with the first mechanism [72].

In Fig. 3d, the possible polymerization mechanisms in the presence of thiols are shown.

These photoinduced reactions follow an orthogonal click chemistry because each available thiol group reacts only once with one alkene double bond, producing homogeneous networks with consistent bulk and local properties [73]. This selectivity can be exploited by performing the reaction in an off-stoichiometric ratio to control the reaction's conversion and still have residual functionalities from the excess component and perform post-printing functionalization [38]. However, the kinetics are dependent on the alkene's reactivity, which increases as the double bond's electron density increases, with norbornene showing the highest reactivity among -ene monomers because of the inherent ring strain [70]. The stability of the intermediate carbon-centred radicals and steric hindrance also influences the reactivity, where terminal -ene groups are usually more reactive.

Regular network formation can be achieved by using multifunctional thiolated cross-linkers with more than two moieties, that can undergo reversible disulfide bond formation as a side reaction when in excess, providing a dynamic behaviour [74]. As mentioned, thiol-ene can be less brittle than (meth)acrylate networks, leading to soft materials and low operational temperatures. Their rigidity can be increased

by exploiting the hydrogen bonding between urethane chains end-capped with norbornene as -ene building blocks [63].

Finally, epoxy can be cured by cationic-induced mechanisms. In this case, the PI generates a cationic active centre after UV light irradiation, which in turns initiates the photopolymerization of epoxy or vinyl ether monomers [75]. Cationic photopolymerization is slower than radical polymerization, but offers some advantages such as reduced shrinkage and residual stresses, which enhances the mechanical properties of the components.[76]

Photoinitiators

A photoinitiation system converts absorbed light into the reactive species to initiate polymerization, as explained previously. The PIs can be either radical or cationic, according to the initiating reactive species that they generate. [62] The absorption wavelength of the selected PI must match the emission of the 3D printer used, to have efficient initiation [81]. On the market, many photoinitiators are available, which, according to their photochemical properties, are activated at different wavelengths, both in the UV, visible and near-infrared light (NIR) ranges (Fig. 4). [82–87]. Most of the radical PIs absorb light in the UV and visible range, which is compatible with all VP techniques, in particular for DLP, that often exploits light emitting at 405 nm. [88] On the other hand, cationic photoinitiators, which need more energetic light sources, are more compatible with SLA, which uses more light sources at 355 nm. [89]

Many photoinitiators belong to Norrish I class. Benzyl ketals are efficient PIs based on the formation of a methyl and benzoyl radical, examples such as 2-hydroxy-2methyl-1-phenyl-propane-1-one (Irgacure 1173) and 2,2-dimethoxy-2-phenylacetophenone (DMPA, Irgacure 651) are used in SLA due to their light absorbance on the UV range. [90] One of the most common benzyl ketals, 2-hydroxy-4'-(2-hydroxyethoxy)-2-methylpropiophenone (Irgacure 2959) has a hydrophilic nature due to its hydroethoxy group and does not produce harmful by-products, making it compatible with cells [91].

Instead, phosphine oxide PIs present lower energy levels in their excited states because of the proximity of the phosphorous atom to the carbonyl group, absorbing wavelengths around 400 nm, preferable on DLP [92, 93]. Acyl phosphine oxides, such as diphenyl(2,4,6-trimethylbenzoyl)phosphine oxide (MAPO or TPO) and *bis*(2,4,6-trimethylbenzoyl)phenylphosphine oxide (Irgacure 819, BAPO) provide photosensitivity in the wavelengths 380–450 nm, and generate radicals under visible light irradiation [94–96].

As introduced in the previous section, Norrish II photoinitiators can also be employed. Norrish type II PIs differ from type I PIs in a bimolecular process. They produce free radicals through direct hydrogen abstraction or electron transfer once it reaches the excited triplet states under light exposure in the presence of a co-initiator
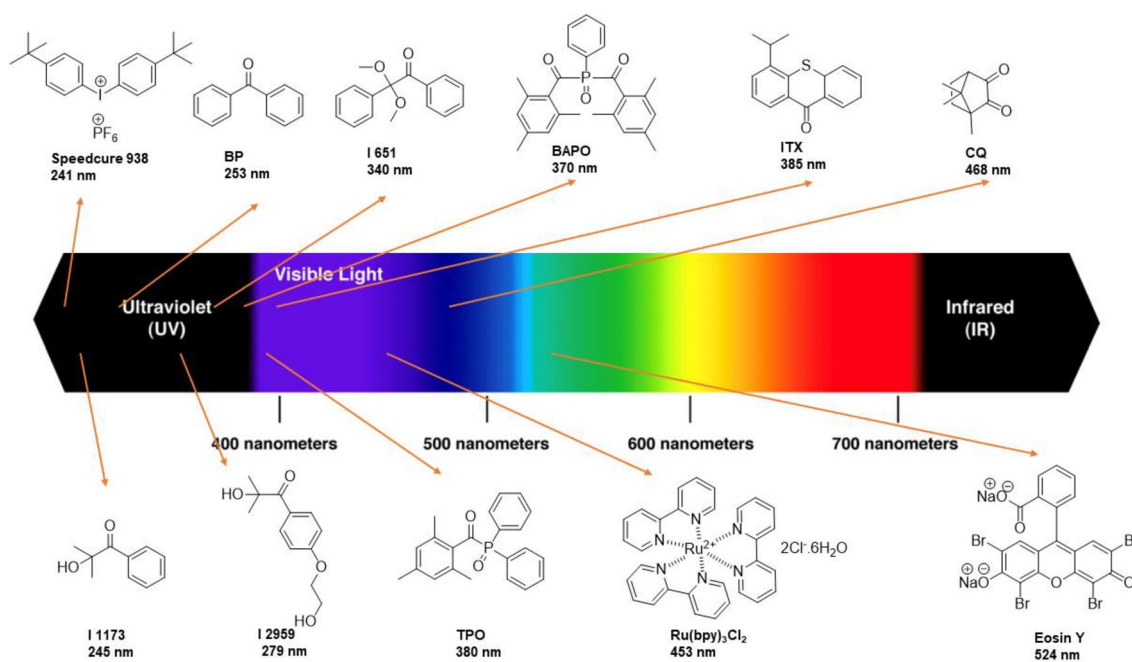

Fig. 4 PI absorption. Chemical structures and maximum absorption wavelength of the recalled PIs used for 3D photopolymerization. Some of these PIs have multiple absorption peaks

(COI) or synergist [97] (Eq. 2). For instance, the most common photosensitizers are camphorquinone (CQ) and benzophenone (BP), and isopropyltyhioxanthone (ITX) and COI are usually tertiary amines, that produce stable radicals [98]. Considering chemical stability and blocking effects, type II PIs possess more advantages for initiating polymerization, but as drawbacks, these systems suffer from poor water solubility, low reactivity, a tendency for discolouration and the inclusion of volatile and odorous amines [99, 100].

Additionally, Eosin Y can be considered a cytocompatible [101] visible-light type II PI. This is a xanthene dye used for histological staining, absorbing light from 490 to 650 nm, requiring both a tertiary amine as COI and a nitrogen-containing monomer (1-vinyl-2 pyrrolidinone NVP) to react [161].

Besides Norrish-type reactions, PIs for redox reactions are also reported, where Eosin Y has been used without the need for a COI [100]. The excited PI oxidizes phenolic tyramine groups into tyrosyl radicals, which form dityrosine bonds from nearby tyrosine groups and are cross-linked in a tyramine network [102]. Moreover, organometallic complexes are included in this category, as tris(2,2'-bipyridyl)-ruthenium(II) chloride hexahydrate ([Ru(II)(bpy)$_3$]Cl$_2$). It has strong visible light absorption, relatively long-lived excited states and suitable redox potentials [103]. Ru(II) complexes are water soluble and in joining with a persulphate can accept electrons when Ru is photoexcited to a triple state [104]. Once the Ru(III) is formed, the persulphate dissociates into sulphate radicals that follow the free-radical or thiol-ene chain polymerization.

Regarding the cationic process, the most commonly used PIs are diazonium salts, diaryliodonium salts as the *Bis*-(4-t-butylphenyl)-iodonium hexafluorophosphate (Speedcure 938) [77], triarylsulfonium salts, alkylsulfonium salts, iron arene salt, sulfonyloxyketone and triarylsiloxane. While the monomers suitable for this mechanism are mainly epoxy, vinyl ethers, lactones, acetals, cyclic ethers, etc.

The activation of the onium salts involves the photoexcitation and decay of the resulting excited singlet state, with both heterolytic and homolytic cleavages [78]. The generated cationic radicals are aryl and aryliodine cations generated during photolysis that further react with the components on the formulations, mainly monomers, to give Brønsted acids which are the predominant initiators [50, 79, 80]. The strength of this acid is the key to determining whether and how the polymerization proceeds. If the acid is not strong enough, the paired anion has a strong nucleophilicity and is easily combined with the carbon cationic centre to prevent polymerization proceeding.

Dyes in VP

In 3DP technologies, the fundamental roles of the dye are printability and resolution. Generally, dyes are used as additives for controlling the polymerization, fundamental for high-fidelity printing and for avoiding a loss of features and precision by attenuating light absorption. However, their use results in an undesired final colour or, in some cases, are applied only for aesthetic aspects [44].

Dyes are typically UV and visible light absorbers (e.g. azobenzenes, benzotriazoles families). These additives can be dispersed in the liquid formulation or covalently linked to the monomer/polymer chains. [9, 105] The most common dyes are listed in Table 1.

The selection of the correct dye must be done considering the absorption spectrum of the used photoinitiator and the dye, and the emission wavelength of the printing machine. Commonly, the photoinitiators absorb in a similar working range to the 3D printing machines, e.g. around 355 nm for some SL lasers, to 385/405 for common DLP. For this reason, in general the dyes also absorb in the UV range or at wavelengths below 500 nm. [18] Sudan I is probably the most common photoabsorber, and its use has been thoroughly investigated to limit the curing depth and obtain better Z-resolution [45, 111, 116].
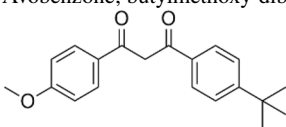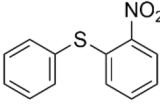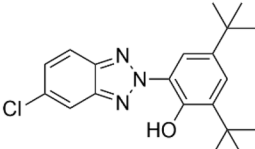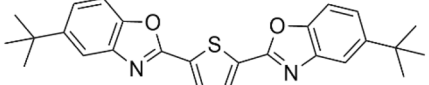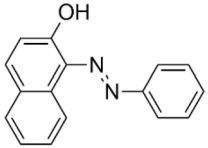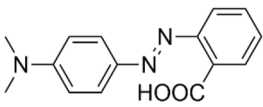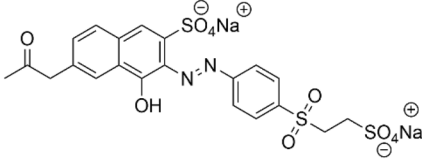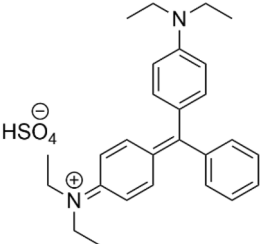
Fillers

The addition of fillers is the most common strategy to overcome polymeric materials limitations, to introduce controlled anisotropy or obtain specific properties such as electrical or thermal conductivity, luminescence, stiffness, electromagnetic shielding or antibacterial properties. In addition, fillers can reduce the shrinkage and consequently result in better accuracy. [118–124] The main function of the fillers can be observed in Fig. 5.

The use of carbon materials (e.g. graphene, nanotubes), ceramic and metal powders, and glassy and fibrous materials (e.g. cellulose) as fillers reinforce the structure and improve mechanical properties. Meanwhile, to improve thermal, chemical and UV resistance, the most common fillers are minerals (e.g. titanium) and bio-fillers (e.g. coffee grounds, wood flour) [125].

In some cases, the filler content can be higher than the main matrix material turns out to be the principal component. The selection of the filler should be done taking into account that the composite resin must be stable during the process. This means a stable and homogeneous suspension that does not suffer with sedimentation, agglomeration or collateral reactions. [122, 126] Additionally, the fillers cannot present excessive absorption that compromises the transparency of the blend or generates scattering phenomena.

Table 1 List of most common dyes used in VP 3D printing

Dye names and structure	λ_{max} (nm)	Concentration reported in literature and application[a]
Avobenzone; butylmethoxy-dibenzoyl-methane	357	0.38 wt% in PEGDA; biomedical applications [106]
		1% in PEGDA; microfluidics channels [107]
2-nitrophenyl phenyl sulfide (NPS)	360	2 wt% in PEGDA [106]; microfluidics channels [107] and microchannels [108]
Tinuvin 327; 2-(2′-Hydroxy-3′,5′-di-tert-butyl-phenyl)-5-chlorobenzo-triazole	365	0–0.15 wt % in IBXA HDDA /BEDA mixture; 3D microstructures [109]
Benetex OB; 2,2'-(2,5-thiophenediyl)bis(5-tert-butylbenzoxazole)	375; 435	0.25% in PEGDA; microfluidics channels [107]
Sudan I; solvent yellow 14; solvent orange R	418; 476	~4 wt% in PEGDA; improved printing resolution [110]
		0.1–0.5 wt% in commercial elastomer; TangoPlus, miniaturized soft robotics [111]
		~0.014 wt% in PEGDMA; antimicrobial hydrogel scaffolds [112]
		0–0.25 wt % in acrylate/allyl/ thiol mixture; uniformity study [45]
Methyl red; acid red 2	410; 520 (pH < 4.4)	0.05 wt% in bio-based acrylate monomer; high printing resolution [113]
		0.2 wt% in starch; hydrogels [114]
		0.1 wt% in phosphorescent bio-based resin [115]
Reactive orange 16; remazol; Brilliant orange 3R	388; 494	0.063–0.25 wt.% in PEGDA/AETAC mixture; monolithic ion absorbers [116]
		0.2 wt% in PEGDA; precise conductive structures [93]
		0.2 wt% in BEDA; microcantilever [94]
Brilliant green; diamond green; Emerald green; ethyl green	650; 440	0.2 wt% in PEGDA/CNC; hydrogel [117]

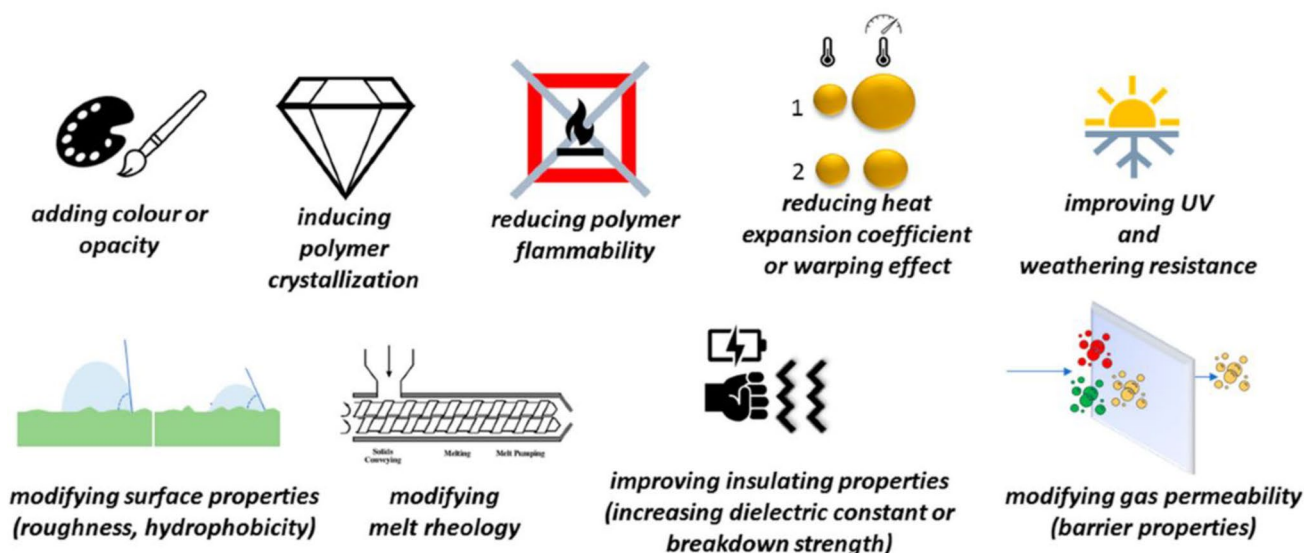[a]Proportional to the monomer

Fig. 5 Different functions of fillers in polymeric mixtures. Reprinted from [125]

Based on the composition, fillers can be divided into organic and inorganic types. The organic types are represented by natural polymers (e.g. cellulose), generally with an intrinsic fibrillar structure [127] and synthetic polymers (polyamide or polyester). Inorganic compounds include oxides and hydroxides ($Al(OH)_3$, $Mg(OH)_2$, TiO_2, Fe_3O_4), salts ($CaCO_3$, $BaSO_4$), metals and silicates [125].

Radical scavengers

A radical scavenger is a chemical substance added to a polymer mixture to remove or de-activate impurities and undesired reaction products. The polymeric radical scavengers are desired as easily separable antioxidants or as films having antioxidation activity. For instance, to improve the storage stability of a rubber formulation, a radical scavenger can be applied to reduce premature cross-linking reactions under dark conditions. [128] Tocopherol and naringenin are other free-radical scavengers that act as antioxidants or synthetic catalytic scavengers.

Conclusions

Three-dimensional printing plays an important role in research, industry and daily life. Among the various 3D printing technologies, light-based 3D methods (SL, DLP, CLIP, etc.) represent an intriguing option because they can combine fast printing times with high complexity and superior precision of the printed objects. Furthermore, these techniques allow local control of chemical–physical properties since it is possible to tune the ink properties. In this context, the chemistry beyond the development of photocurable formulation is much more complicated than in the development of 3D printable materials suitable for other technologies, and it needs to be fully understood.

For the scope of this article, the chemistry beyond light-induced 3D printing is presented, describing the roles and effects of the various ingredients necessary to develop 3D printable formulations. Furthermore, how these interact with each other and how the user can alter the formulation to obtain high printability and the desired properties are described. The tools here provided offer a plethora of strategies that can be implemented and exploited in different areas. For instance, for a chemist who would like to test newly synthesized photocompounds in 3D printable materials, replacing photoinitiating systems, it is important to know that photoactivicty is not the only requirement, but it must also go with control of the extent of polymerization. Alternatively, an engineer who wants to implement device properties by altering local functionalities, and thus changing the monomers, must be aware that not all the monomers can efficiently co-polymerize in different layers due to differences in the reactivity of surface energy. In both cases, it is necessary to have a deep understanding of 3D printing, from a general perspective, which goes from chemistry to device properties, as described here.

Declarations

Conflicts of interest There are no conflicts to declare.

References

1. Jones N (2012) Science in three dimensions: the print revolution. Nature 487(7405):22–23. https://doi.org/10.1038/487022a
2. Gao W, Zhang Y, Ramanujan D, Ramani K, Chen Y, Williams CB et al (2015) The status, challenges, and future of additive manufacturing in engineering. Comput Aided Des 69:65–89. https://doi.org/10.1016/j.cad.2015.04.001
3. Vaneker T, Bernard A, Moroni G, Gibson I, Zhang Y (2020) Design for additive manufacturing: framework and methodology. CIRP Ann 69(2):578–599. https://doi.org/10.1016/j.cirp.2020.05.006
4. Tan LJ, Zhu W, Zhou K (2020) Recent progress on polymer materials for additive manufacturing. Adv Func Mater 30(43):2003062. https://doi.org/10.1002/adfm.202003062
5. Berman B (2012) 3-D printing: the new industrial revolution. Bus Horiz 55(2):155–162. https://doi.org/10.1016/j.bushor.2011.11.003
6. Sanchez-Rexach E, Johnston TG, Jehanno C, Sardon H, Nelson A (2020) Sustainable materials and chemical processes for additive manufacturing. Chem Mater 32(17):7105–7119. https://doi.org/10.1021/acs.chemmater.0c02008
7. Bhatia A, Sehgal AK (2021) Additive manufacturing materials, methods and applications: a review. Mater Today Proc. https://doi.org/10.1016/j.matpr.2021.04.379
8. Oropallo W, Piegl LA (2016) Ten challenges in 3D printing. Eng Comput 32(1):135–148. https://doi.org/10.1007/s00366-015-0407-0
9. Ligon SC, Liska R, Stampfl J, Gurr M, Mülhaupt R (2017) Polymers for 3D printing and customized additive manufacturing. Chem Rev 117(15):10212–10290. https://doi.org/10.1021/acs.chemrev.7b00074
10. Tibbits S (2014) 4D Printing: multi-material shape change. Archit Des 84(1):116–121. https://doi.org/10.1002/ad.1710
11. Pagac M, Hajnys J, Ma Q-P, Jancar L, Jansa J, Stefek P et al (2021) A review of vat photopolymerization technology: materials, applications, challenges, and future trends of 3d printing. Polymers 13(4):598
12. Kodama H (1981) Automatic method for fabricating a three-dimensional plastic model with photo-hardening polymer. Rev Sci Instrum 52(11):1770–1773. https://doi.org/10.1063/1.1136492
13. Hull CW (1985) Apparatus for production of three-dimensional objects by stereolithography. United States
14. Stansbury JW, Idacavage MJ (2016) 3D printing with polymers: challenges among expanding options and opportunities. Dent Mater 32(1):54–64. https://doi.org/10.1016/j.dental.2015.09.018
15. Oesterreicher A, Wiener J, Roth M, Moser A, Gmeiner R, Edler M et al (2016) Tough and degradable photopolymers derived from alkyne monomers for 3D printing of biomedical materials. Polym Chem 7(32):5169–5180. https://doi.org/10.1039/C6PY01132B
16. Ikuta K, Hirowatari K (1993) Real three dimensional micro fabrication using stereo lithography and metal molding. In: Proceedings IEEE Micro Electro Mechanical Systems, pp 42–47
17. Joseph M, Desimone ETS, Alexander E, Philip M (2014) Desimone. Rapid 3D continuous printing of casting molds for metals and other materials
18. Quan H, Zhang T, Xu H, Luo S, Nie J, Zhu X (2020) Photo-curing 3D printing technique and its challenges. Bioactive Materials 5(1):110–115. https://doi.org/10.1016/j.bioactmat.2019.12.003
19. Xing J-F, Zheng M-L, Duan X-M (2015) Two-photon polymerization microfabrication of hydrogels: an advanced 3D printing technology for tissue engineering and drug delivery. Chem Soc Rev 44(15):5031–5039. https://doi.org/10.1039/C5CS00278H
20. Bhattacharya I, Kelly B, Shusteff M, Spadaccini C, Taylor H (2018) Computed axial lithography: volumetric 3D printing of arbitrary geometries (Conference Presentation). SPIE Commercial + Scientific Sensing and Imaging. SPIE
21. Li H, Fan W, Zhu X (2020) Three-dimensional printing: the potential technology widely used in medical fields. J Biomed Mater Res Part A 108(11):2217–2229. https://doi.org/10.1002/jbm.a.36979
22. Enders A, Siller IG, Urmann K, Hoffmann MR, Bahnemann J (2019) 3D printed microfluidic mixers—a comparative study on mixing unit performances. Small 15(2):1804326. https://doi.org/10.1002/smll.201804326
23. Mondschein RJ, Kanitkar A, Williams CB, Verbridge SS, Long TE (2017) Polymer structure-property requirements for stereolithographic 3D printing of soft tissue engineering scaffolds. Biomaterials 140:170–188. https://doi.org/10.1016/j.biomaterials.2017.06.005
24. Ayub NF, Hashim S, Jamaluddin J, Adrus N (2017) New UV LED curing approach for polyacrylamide and poly(N-isopropylacrylamide) hydrogels. New J Chem 41(13):5613–5619. https://doi.org/10.1039/C7NJ00176B
25. Juskova P, Ollitrault A, Serra M, Viovy J-L, Malaquin L (2018) Resolution improvement of 3D stereo-lithography through the direct laser trajectory programming: application to microfluidic deterministic lateral displacement device. Anal Chim Acta 1000:239–247. https://doi.org/10.1016/j.aca.2017.11.062
26. Liu Y, Hu Q, Zhang F, Tuck C, Irvine D, Hague R et al (2016) Additive manufacture of three dimensional nanocomposite based objects through multiphoton fabrication. Polymers 8(9):325
27. Cheng Y-L, Kao H-L (2015) Study on visible-light-curable polycarprolactone and poly(ethylene glycol) diacrylate for LCD-projected maskless additive manufacturing system. SPIE Organic Photonics + Electronics. SPIE
28. Kim SH, Yeon YK, Lee JM, Chao JR, Lee YJ, Seo YB et al (2018) Precisely printable and biocompatible silk fibroin bioink

for digital light processing 3D printing. Nat Commun 9(1):1620. https://doi.org/10.1038/s41467-018-03759-y

29. Yu C, Schimelman J, Wang P, Miller KL, Ma X, You S et al (2020) Photopolymerizable biomaterials and light-based 3D printing strategies for biomedical applications. Chem Rev 120(19):10695–10743. https://doi.org/10.1021/acs.chemrev.9b00810

30. Gonzalez G, Roppolo I, Pirri CF, Chiappone A (2022) Current and emerging trends in polymeric 3D printed microfluidic devices. Add Manufact 55:102867. https://doi.org/10.1016/j.addma.2022.102867

31. Valverde D, Porcar R, Zanatta M, Alcalde S, Altava B, Sans V et al (2022) Towards highly efficient continuous-flow catalytic carbon dioxide cycloadditions with additively manufactured reactors. Green Chem 24(8):3300–3308. https://doi.org/10.1039/D1GC04593H

32. Tumbleston JR, Shirvanyants D, Ermoshkin N, Janusziewicz R, Johnson AR, Kelly D et al (2015) Continuous liquid interface production of 3D objects. Science 347(6228):1349–1352. https://doi.org/10.1126/science.aaa2397

33. Nguyen AK, Narayan RJ (2017) Two-photon polymerization for biological applications. Mater Today 20(6):314–322. https://doi.org/10.1016/j.mattod.2017.06.004

34. Purbrick MD (1996) Photoinitiation, photopolymerization and photocuring. J.-P. Fouassier. Hanser Publishers, Munich, 1995. Polym Int 40(4):315. https://doi.org/10.1002/(SICI)1097-0126(199608)40:4<315::AID-PI566>3.0.CO;2-T.

35. Yagci Y, Jockusch S, Turro NJ (2010) Photoinitiated polymerization: advances, challenges, and opportunities. Macromolecules 43(15):6245–6260. https://doi.org/10.1021/ma1007545

36. Zhou J, Allonas X, Ibrahim A, Liu X (2019) Progress in the development of polymeric and multifunctional photoinitiators. Prog Polym Sci 99:101165. https://doi.org/10.1016/j.progpolymsci.2019.101165

37. Garra P, Fouassier JP, Lakhdar S, Yagci Y, Lalevée J (2020) Visible light photoinitiating systems by charge transfer complexes: Photochemistry without dyes. Prog Polym Sci 107:101277. https://doi.org/10.1016/j.progpolymsci.2020.101277

38. Hoyle CE, Bowman CN (2010) Thiol-ene click chemistry. Angew Chem Int Ed 49(9):1540–1573. https://doi.org/10.1002/anie.200903924

39. From the Preface to the First Edition (1972) In: Van Krevelen DW, Te Nijenhuis K (eds) Properties of Polymers (Fourth Edition). Amsterdam: Elsevier; 2009. p. vii.

40. Nicholson JW (2012) The chemistry of polymers: edition 4. RSC

41. Fouassier JP, Rabek JF (1993) Radiation curing in polymer science and technology: fundamentals and methods Radiation Curing in Polymer Science and Technology. Springer, Dordrecht

42. Ahn D, Stevens LM, Zhou K, Page ZA (2020) Rapid high-resolution visible light 3D printing. ACS Cent Sci 6(9):1555–1563. https://doi.org/10.1021/acscentsci.0c00929

43. Xiao P, Zhang J (2021) 3D Printing with Light, Berlin, Boston: De Gruyter. https://doi.org/10.1515/97831105705883D

44. Gastaldi M, Cardano F, Zanetti M, Viscardi G, Barolo C, Bordiga S et al (2021) Functional dyes in polymeric 3D printing: applications and perspectives. ACS Mater Lett 3(1):1–17. https://doi.org/10.1021/acsmaterialslett.0c00455

45. Vitale A, Cabral JT (2016) Frontal conversion and uniformity in 3D printing by photopolymerisation. Mater (Basel Switzerl) 9(9):760. https://doi.org/10.3390/ma9090760

46. Lin J-T, Liu H-W, Chen K-T, Cheng D-C (2019) Modeling the kinetics, curing depth, and efficacy of radical-mediated photopolymerization: the role of oxygen inhibition, viscosity, and dynamic light intensity. Front Chem 7:760

47. Cook CC, Fong EJ, Schwartz JJ, Porcincula DH, Kaczmarek AC, Oakdale JS et al (2020) Highly tunable thiol-ene photoresins for volumetric additive manufacturing. Adv Mater 32(47):2003376. https://doi.org/10.1002/adma.202003376

48. He Y, Li N, Xiang Z, Rong Y, Zhu L, Huang X (2022) Natural polyphenol as radical inhibitors used for DLP-based 3D printing of photosensitive gels. Mater Today Commun 33:104698. https://doi.org/10.1016/j.mtcomm.2022.104698

49. Layani M, Wang X, Magdassi S (2018) Novel materials for 3D printing by photopolymerization. Adv Mater 30(41):1706344. https://doi.org/10.1002/adma.201706344

50. Crivello JV, Reichmanis E (2014) Photopolymer materials and processes for advanced technologies. Chem Mater 26(1):533–548. https://doi.org/10.1021/cm402262g

51. Appuhamillage GA, Chartrain N, Meenakshisundaram V, Feller KD, Williams CB, Long TE (2019) 110th anniversary: vat photopolymerization-based additive manufacturing: current trends and future directions in materials design. Ind Eng Chem Res 58(33):15109–15118. https://doi.org/10.1021/acs.iecr.9b02679

52. Lee M, Rizzo R, Surman F, Zenobi-Wong M (2020) Guiding lights: tissue bioprinting using photoactivated materials. Chem Rev 120(19):10950–11027. https://doi.org/10.1021/acs.chemrev.0c00077

53. Samadian H, Maleki H, Allahyari Z, Jaymand M (2020) Natural polymers-based light-induced hydrogels: promising biomaterials for biomedical applications. Coord Chem Rev 420:213432. https://doi.org/10.1016/j.ccr.2020.213432

54. Bagheri A, Jin J (2019) Photopolymerization in 3D Printing. ACS Appl Polym Mater 1(4):593–611. https://doi.org/10.1021/acsapm.8b00165

55. Ng WL, Lee JM, Zhou M, Chen Y-W, Lee K-XA, Yeong WY et al (2020) Vat polymerization-based bioprinting—process, materials, applications and regulatory challenges. Biofabrication 12(2):022001. https://doi.org/10.1088/1758-5090/ab6034

56. Jean Pierre Fouassier JL (2012) Photoinitiators for polymer synthesis: scope, reactivity and efficiency. Wiley-VCH Verlag GmbH & Co. KGaA

57. Narupai B, Nelson A (2020) 100th anniversary of macromolecular science viewpoint: macromolecular materials for additive manufacturing. ACS Macro Lett 9(5):627–638. https://doi.org/10.1021/acsmacrolett.0c00200

58. Lammel-Lindemann J, Dourado IA, Shanklin J, Rodriguez CA, Catalani LH, Dean D (2020) Photocrosslinking-based 3D printing of unsaturated polyesters from isosorbide: a new material for resorbable medical devices. Bioprinting. https://doi.org/10.1016/j.bprint.2019.e00062

59. Scott PJ, Meenakshisundaram V, Hegde M, Kasprzak CR, Winkler CR, Feller KD et al (2020) 3D Printing latex: a route to complex geometries of high molecular weight polymers. ACS Appl Mater Interfaces 12(9):10918–10928. https://doi.org/10.1021/acsami.9b19986

60. Leonards H, Engelhardt S, Hoffmann A, Pongratz L, Schriever S, Bläsius J, et al (2015) Advantages and drawbacks of Thiolene based resins for 3D-printing. SPIE LASE. SPIE

61. Zhao T, Li X, Yu R, Zhang Y, Yang X, Zhao X et al (2018) Silicone–Epoxy-based hybrid photopolymers for 3D printing. Macromol Chem Phys 219(10):1700530. https://doi.org/10.1002/macp.201700530

62. Zhang J, Xiao P (2018) 3D printing of photopolymers. Polym Chem 9(13):1530–1540. https://doi.org/10.1039/C8PY00157J

63. Lu H, Carioscia JA, Stansbury JW, Bowman CN (2005) Investigations of step-growth thiol-ene polymerizations for novel dental restoratives. Dent Mater 21(12):1129–1136. https://doi.org/10.1016/j.dental.2005.04.001

64. Chen L, Wu Q, Wei G, Liu R, Li Z (2018) Highly stable thiol–ene systems: from their structure–property relationship to DLP 3D printing. J Mater Chem C 6(43):11561–11568. https://doi.org/10.1039/C8TC03389G

65. Dillman BF (2013) The kinetics and physical properties of epoxides, acrylates, and hybrid epoxy-acrylate photopolymerization systems. In: The kinetics and physical properties of epoxides, acrylates, and hybrid epoxy-acrylate photopolymerization systems: University of Iowa

66. Sycks DG, Wu T, Park HS, Gall K (2018) Tough, stable spiroacetal thiol-ene resin for 3D printing. J Appl Polym Sci 135(22):46259. https://doi.org/10.1002/app.46259

67. Beuermann S, Paquet DA, McMinn JH, Hutchinson RA (1996) Determination of free-radical propagation rate coefficients of butyl, 2-ethylhexyl, and dodecyl acrylates by pulsed-laser polymerization. Macromolecules 29(12):4206–4215. https://doi.org/10.1021/ma960081c

68. Choi JR, Yong KW, Choi JY, Cowie AC (2019) Recent advances in photo-crosslinkable hydrogels for biomedical applications. Biotechniques 66(1):40–53. https://doi.org/10.2144/btn-2018-0083

69. Kannurpatti AR, Anseth JW, Bowman CN (1998) A study of the evolution of mechanical properties and structural heterogeneity of polymer networks formed by photopolymerizations of multifunctional (meth)acrylates. Polymer 39:2507–2513

70. Nair DP, Cramer NB, Scott TF, Bowman CN, Shandas R (2010) Photopolymerized thiol-ene systems as shape memory polymers. Polymer 51(19):4383–4389. https://doi.org/10.1016/j.polymer.2010.07.027

71. Nair DP, Podgórski M, Chatani S, Gong T, Xi W, Fenoli CR et al (2014) The thiol-michael addition click reaction: a powerful and widely used tool in materials chemistry. Chem Mater 26(1):724–744. https://doi.org/10.1021/cm402180t

72. Hoyle CE, Lee TY, Roper T (2004) Thiol–enes: chemistry of the past with promise for the future. J Polym Sci Part A: Polym Chem 42(21):5301–5338. https://doi.org/10.1002/pola.20366

73. Bertlein S, Brown G, Lim KS, Jungst T, Boeck T, Blunk T et al (2017) Thiol-ene clickable gelatin: a platform bioink for multiple 3d biofabrication technologies. Adv Mater 29(44):1703404. https://doi.org/10.1002/adma.201703404

74. Rydholm AE, Reddy SK, Anseth KS, Bowman CN (2006) Controlling network structure in degradable thiol−acrylate biomaterials to tune mass loss behavior. Biomacromol 7(10):2827–2836. https://doi.org/10.1021/bm0603793

75. Shi Y, Yan C, Zhou Y, Wu J, Wang Y, Yu S et al (2021) Chapter 3—polymer materials for additive manufacturing: liquid materials. In: Shi Y, Yan C, Zhou Y, Wu J, Wang Y, Yu S et al (eds) Materials for additive manufacturing. Academic Press, pp 191–359

76. Sangermano M, Razza N, Crivello JV (2014) Cationic UV-curing: technology and applications. Macromol Mater Eng 299(7):775–793. https://doi.org/10.1002/mame.201300349

77. Villotte S, Gigmes D, Dumur F, Lalevée J (2019) Design of iodonium salts for UV or near-UV LEDs for photoacid generator and polymerization purposes. Molecules. https://doi.org/10.3390/molecules25010149

78. Sangermano M, Roppolo I, Chiappone A (2018) New Horizons in Cationic Photopolymerization. Polymers 10(2):136

79. Peter Pappas S, Pappas BC, Gatechair LR, Jilek JH, Schnabel W (1984) Photoinitiation of cationic polymerization. IV. Direct and sensitized photolysis of aryl iodonium and sulfonium salts. Polym Photochem 5(1):1–22. https://doi.org/10.1016/0144-2880(84)90018-6

80. Yağci Y, Reetz I (1998) Externally stimulated initiator systems for cationic polymerization. Prog Polym Sci 23(8):1485–1538. https://doi.org/10.1016/S0079-6700(98)00010-0

81. Ikemura K, Endo T (2010) A review of the development of radical photopolymerization initiators used for designing light-curing dental adhesives and resin composites. Dent Mater J 29(5):481–501. https://doi.org/10.4012/dmj.2009-137

82. Shanmugam S, Xu J, Boyer C (2016) Light-regulated polymerization under near-infrared/far-red irradiation catalyzed by Bacteriochlorophyll a. Angew Chem Int Ed 55(3):1036–1040. https://doi.org/10.1002/anie.201510037

83. Corrigan N, Xu J, Boyer C (2016) A photoinitiation system for conventional and controlled radical polymerization at visible and NIR wavelengths. Macromolecules 49(9):3274–3285. https://doi.org/10.1021/acs.macromol.6b00542

84. Al Mousawi A, Poriel C, Dumur F, Toufaily J, Hamieh T, Fouassier JP et al (2017) Zinc tetraphenylporphyrin as high performance visible light photoinitiator of cationic photosensitive resins for LED projector 3D printing applications. Macromolecules 50(3):746–753. https://doi.org/10.1021/acs.macromol.6b02596

85. Zhang J, Lalevée J, Zhao J, Graff B, Stenzel MH, Xiao P (2016) Dihydroxyanthraquinone derivatives: natural dyes as blue-light-sensitive versatile photoinitiators of photopolymerization. Polym Chem 7(47):7316–7324. https://doi.org/10.1039/C6PY01550F

86. Hong BM, Park SA, Park WH (2019) Effect of photoinitiator on chain degradation of hyaluronic acid. Biomater Res 23(1):21. https://doi.org/10.1186/s40824-019-0170-1

87. Xu J, Shanmugam S, Fu C, Aguey-Zinsou K-F, Boyer C (2016) Selective photoactivation: from a single unit monomer insertion reaction to controlled polymer architectures. J Am Chem Soc 138(9):3094–3106. https://doi.org/10.1021/jacs.5b12408

88. Fouassier JP, Allonas X, Burget D (2003) Photopolymerization reactions under visible lights: principle, mechanisms and examples of applications. Prog Org Coat 47(1):16–36. https://doi.org/10.1016/S0300-9440(03)00011-0

89. Sangermano M (2012) Advances in cationic photopolymerization. Pure Appl Chem 84(10):2089–2101. https://doi.org/10.1351/PAC-CON-12-04-11

90. Fischer H, Radom L (2001) Factors controlling the addition of carbon-centered radicals to alkenes—an experimental and theoretical perspective. Angew Chem Int Ed 40(8):1340–1371. https://doi.org/10.1002/1521-3773(20010417)40:8%3c1340::AID-ANIE1340%3e3.0.CO;2-%23

91. Lavker R, Kaidbey K (1997) The spectral dependence for UVA-induced cumulative damage in human skin. J Invest Dermatol 108(1):17–21. https://doi.org/10.1111/1523-1747.ep12285613

92. Fantino E, Chiappone A, Calignano F, Fontana M, Pirri F, Roppolo I (2016) In situ thermal generation of silver nanoparticles in 3D printed polymeric structures. Materials 9(7):589

93. Fantino E, Chiappone A, Roppolo I, Manfredi D, Bongiovanni R, Pirri CF et al (2016) 3D printing of conductive complex structures with in situ generation of silver nanoparticles. Adv Mater 28(19):3712–3717. https://doi.org/10.1002/adma.201505109

94. Stassi S, Fantino E, Calmo R, Chiappone A, Gillono M, Scaiola D et al (2017) Polymeric 3D printed functional microcantilevers for biosensing applications. ACS Appl Mater Interfaces 9(22):19193–19201. https://doi.org/10.1021/acsami.7b04030

95. Patel DK, Sakhaei AH, Layani M, Zhang B, Ge Q, Magdassi S (2017) Highly stretchable and UV curable elastomers for digital light processing based 3D printing. Adv Mater 29(15):1606000. https://doi.org/10.1002/adma.201606000

96. Shukrun E, Cooperstein I, Magdassi S (2018) 3D-printed organic-ceramic complex hybrid structures with high silica content. Adv Sci 5(8):1800061. https://doi.org/10.1002/advs.201800061

97. Dietliker K, Hüsler R, Birbaum JL, Ilg S, Villeneuve S, Studer K et al (2007) Advancements in photoinitiators—opening up new

applications for radiation curing. Prog Org Coat 58(2):146–157. https://doi.org/10.1016/j.porgcoat.2006.08.021

98. Lalevée J, Fouassier JP, Graff B, Zhang J, Xiao P (2018) Chapter 6 how to design novel photoinitiators for blue light. In: Photopolymerisation Initiating Systems. The Royal Society of Chemistry, p. 179–199.

99. Jauk S, Liska R (2005) Photoinitiators with functional groups, 8. Macromol Rapid Commun 26(21):1687–1692. https://doi.org/10.1002/marc.200500507

100. Fors BP, Hawker CJ (2012) Control of a living radical polymerization of methacrylates by light. Angew Chem Int Ed 51(35):8850–8853. https://doi.org/10.1002/anie.201203639

101. Shih H, Lin C-C (2013) Visible-light-mediated thiol-ene hydrogelation using Eosin-Y as the only photoinitiator. Macromol Rapid Commun 34(3):269–273. https://doi.org/10.1002/marc.201200605

102. Ohtsuki A, Goto A, Kaji H (2013) Visible-light-induced reversible complexation mediated living radical polymerization of methacrylates with organic catalysts. Macromolecules 46(1):96–102. https://doi.org/10.1021/ma302244j

103. Lim KS, Schon BS, Mekhileri NV, Brown GCJ, Chia CM, Prabakar S et al (2016) New visible-light photoinitiating system for improved print fidelity in gelatin-based bioinks. ACS Biomater Sci Eng 2(10):1752–1762. https://doi.org/10.1021/acsbiomaterials.6b00149

104. Lim KS, Klotz BJ, Lindberg GCJ, Melchels FPW, Hooper GJ, Malda J et al (2019) Visible light cross-linking of gelatin hydrogels offers an enhanced cell microenvironment with improved light penetration depth. Macromol Biosci 19(6):1900098. https://doi.org/10.1002/mabi.201900098

105. Gürses A, Açıkyıldız M, Güneş K, Gürses MS (2016) Dyes and pigments: their structure and properties. In: Gürses A, Açıkyıldız M, Güneş K, Gürses MS (eds) Dyes and Pigments. Springer International Publishing, Cham, pp 13–29

106. Warr C, Valdoz JC, Bickham BP, Knight CJ, Franks NA, Chartrand N et al (2020) Biocompatible PEGDA Resin for 3D Printing. ACS Appl Bio Mater 3(4):2239–2244. https://doi.org/10.1021/acsabm.0c00055

107. Gong H, Bickham BP, Woolley AT, Nordin GP (2017) Custom 3D printer and resin for 18 μm × 20 μm microfluidic flow channels. Lab Chip 17(17):2899–2909. https://doi.org/10.1039/C7LC00644F

108. Gong H, Woolley AT, Nordin GP (2018) 3D printed high density, reversible, chip-to-chip microfluidic interconnects. Lab Chip 18(4):639–647. https://doi.org/10.1039/C7LC01113J

109. Choi J-W, Wicker RB, Cho S-H, Ha C-S, Lee S-H (2009) Cure depth control for complex 3D microstructure fabrication in dynamic mask projection microstereolithography. Rapid Prototyp J 15(1):59–70. https://doi.org/10.1108/13552540910925072

110. Lee MP, Cooper GJT, Hinkley T, Gibson GM, Padgett MJ, Cronin L (2015) Development of a 3D printer using scanning projection stereolithography. Sci Rep 5(1):9875. https://doi.org/10.1038/srep09875

111. Zhang Y-F, Ng CJ-X, Chen Z, Zhang W, Panjwani S, Kowsari K et al (2019) Miniature pneumatic actuators for soft robots by high-resolution multimaterial 3D printing. Adv Mater Technol 4(10):1900427. https://doi.org/10.1002/admt.201900427

112. Garcia C, Gallardo A, López D, Elvira C, Azzahti A, Lopez-Martinez E et al (2018) Smart pH-responsive antimicrobial hydrogel scaffolds prepared by additive manufacturing. ACS Appl Bio Mater 1(5):1337–1347. https://doi.org/10.1021/acsabm.8b00297

113. Cosola A, Conti R, Grützmacher H, Sangermano M, Roppolo I, Pirri CF et al (2020) Multiacrylated cyclodextrin: a bio-derived photocurable macromer for VAT 3D printing. Macromol Mater Eng 305(9):2000350. https://doi.org/10.1002/mame.202000350

114. Noè C, Tonda-Turo C, Chiappone A, Sangermano M, Hakkarainen M (2020) Light processable starch hydrogels. Polymers 12(6):1359. https://doi.org/10.3390/polym12061359

115. Maturi M, Pulignani C, Locatelli E, Vetri Buratti V, Tortorella S, Sambri L et al (2020) Phosphorescent bio-based resin for digital light processing (DLP) 3D-printing. Green Chem 22(18):6212–6224. https://doi.org/10.1039/D0GC01983F

116. Simon U, Dimartino S (2019) Direct 3D printing of monolithic ion exchange adsorbers. J Chromatogr A 1587:119–128. https://doi.org/10.1016/j.chroma.2018.12.017

117. Wang J, Chiappone A, Roppolo I, Shao F, Fantino E, Lorusso M et al (2018) All-in-one cellulose nanocrystals for 3D printing of nanocomposite hydrogels. Angew Chem Int Ed 57(9):2353–2356. https://doi.org/10.1002/anie.201710951

118. Gonzalez G, Chiappone A, Roppolo I, Fantino E, Bertana V, Perrucci F et al (2017) Development of 3D printable formulations containing CNT with enhanced electrical properties. Polymer 109:246–253. https://doi.org/10.1016/j.polymer.2016.12.051

119. Hu G, Cao Z, Hopkins M, Lyons JG, Brennan-Fournet M, Devine DM (2019) Nanofillers can be used to enhance the thermal conductivity of commercially available SLA resins. Proc Manufact 38:1236–1243. https://doi.org/10.1016/j.promfg.2020.01.215

120. Frascella F, González G, Bosch P, Angelini A, Chiappone A, Sangermano M et al (2018) Three-dimensional printed photoluminescent polymeric waveguides. ACS Appl Mater Interfaces 10(45):39319–39326. https://doi.org/10.1021/acsami.8b16036

121. Tan HW, An J, Chua CK, Tran T (2019) Metallic nanoparticle inks for 3D printing of electronics. Adv Electron Mater 5(5):1800831. https://doi.org/10.1002/aelm.201800831

122. Taormina G, Sciancalepore C, Messori M, Bondioli F (2018) 3D printing processes for photocurable polymeric materials: technologies, materials, and future trends. J Appl Biomater Funct Mater 16(3):151–160. https://doi.org/10.1177/2280800018764770

123. Wang X, Jiang M, Zhou Z, Gou J, Hui D (2017) 3D printing of polymer matrix composites: a review and prospective. Compos B Eng 110:442–458. https://doi.org/10.1016/j.compositesb.2016.11.034

124. Khalifa M, Anandhan S, Wuzella G, Lammer H, Mahendran AR (2020) Thermoplastic polyurethane composites reinforced with renewable and sustainable fillers—a review. Polym Plast Technol Mater 59(16):1751–1769. https://doi.org/10.1080/25740881.2020.1768544

125. Sztorch B, Brząkalski D, Pakuła D, Frydrych M, Špitalský Z, Przekop RE (2022) Natural and synthetic polymer fillers for applications in 3D printing-FDM technology area. Solids 3(3):508–548

126. Angelopoulos PM, Samouhos M, Taxiarchou M (2021) Functional fillers in composite filaments for fused filament fabrication; a review. Mater Today Proc 37:4031–4043. https://doi.org/10.1016/j.matpr.2020.07.069

127. Mazzanti V, Malagutti L, Mollica F (2019) FDM 3D printing of polymers containing natural fillers: a review of their mechanical properties. Polymers 11(7):1094

128. Strohmeier L, Frommwald H, Schlögl S (2020) Digital light processing 3D printing of modified liquid isoprene rubber using thiol-click chemistry. RSC Adv 10(40):23607–23614. https://doi.org/10.1039/D0RA04186F

Publisher's Note Springer Nature remains neutral with regard to jurisdictional claims in published maps and institutional affiliations.